



Center for Optical Technologies Biophotonics Group Research Activities, 2011

Direct Enumeration of Dilute Bio-Nanoparticles in an Optical Trap: Yi Hu, Xuanhong Cheng and H. Daniel Ou-Yang (hdo0@lehigh.edu) *Lehigh University*. Observation and real time quantification of bio-nanoparticles such as virions is significant for clinical diagnosis, environmental monitoring and fundamental science. However, the low concentration of these particles in their natural environment often prevents direct detection. Using optical trapping, we shown in our prior work that dilute nanoparticle concentration increases with trapping laser power, following a Boltzmann distribution $N_{trap}/N_0 = \exp(U_{trap}/k_B T)$. Here we demonstrate that the concentration of nanoparticles in the optical trap can be determined by fluorescence correlation spectroscopy (FCS). This methodology is tested on Gag virus-like particle (VLPs) in cell medium suspension. We anticipate the methodology described in this article will have potential application on biological suspension.

and an exponential fitting (red solid line) shows the trapping energy per particle is $0.02 k_B T$ at each milli-Watts of laser power.

Mapping the Optical Trapping Energy of Nanoparticles in an Optical Bottles via Confocal Microscopy: Melissa Goleb, H. Daniel Ou-Yang (hdo0@lehigh.edu) *Lehigh University*. Optical trapping of nanoparticles, since its discovery by Ashkin et. al. in 1986, has become one of the most promising techniques in optical technology for nanoparticle manipulation. Using an infrared laser setup, we have the potential to contain nanoparticles with diameters as small as 100 nm in a centralized area. The area of containment of several of these particles is called an optical bottle. Optical traps and bottles allow control over nanoparticles that were difficult to manipulate before due to their size. One of the key parameters of optical traps is the trapping energy that correlates to how strongly the nanoparticles are attracted to the area. Trapping energy or the depth of the potential well of the trap can be determined by an ensemble method proposed by Junio et. al. This method has been expanded upon to create a method through which we are able to measure the trapping potential well in two dimensions. For a particle to be considered as stably trapped, the gradient force of the laser must be greater than the scattering force from the particles in all directions. After ensuring that the gradient force is large enough, we can assume the particles tend to stay within the area of the optical bottle. From this we can then map the profile of the bottle and analyze the potential energy well as a function of the distance from the center of the trap. With this research we are mapping only the 2D energy profile of the trap, but even with this information we can learn more about optical traps. This research can lead to better methods of concentrating nanoparticles by light to improve the sensitivity of diagnostics pathogens for biomedical applications.

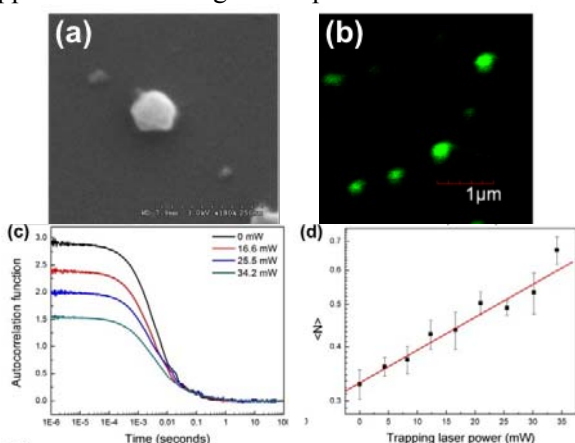


Fig. (a) SEM image of Gag VLP, the diameter is measured to be 110 nm. (b) Fluorescent image of Gag VLP under 100X objective. (c) Selected autocorrelation curves of VLPs in culture medium at different trapping laser power. The prefactor of ACF decreases as the trapping laser power increases. (d) The average number of particles in the observation volume is plotted versus the trapping laser power,

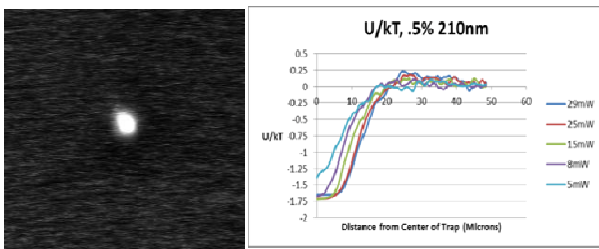


Fig. (Left) An image of an optical bottle, taken with a confocal microscope setup. (Right) The corresponding graphical output of distance from the center of the trap vs. potential trapping energy, calculated using the ensemble method originated in Junio et al.

Optical Trapping of Gold Nanoparticles by Dark Field Microscopy: Lin Ling¹, Jinxin Fu^{1,2}, Honglian Guo¹ and H. Daniel Ou-Yang² (hdo0@Lehigh.edu)
¹Chinese Academy of Sciences, Beijing, ²Lehigh University. Observation and trapping of nano-sized particles have been a challenge over the decades. For metal nanoparticles, because of the existence of localized surface plasmon resonance (LSP), the near-field electro-magnetic field is enhanced. In this work, we used a dark field microscope, combined with double optical tweezers system, to study the dynamics of gold nanoparticles in an optical trap. We observed the trapping of nanoparticles and found that dilute gold nanoparticles are trapped one after another, as shown in Fig. top. Moreover, we confirmed that the orientation of trapped gold nanorods is directly related to the polarization of the trapping beam (shown in Fig. bottom).

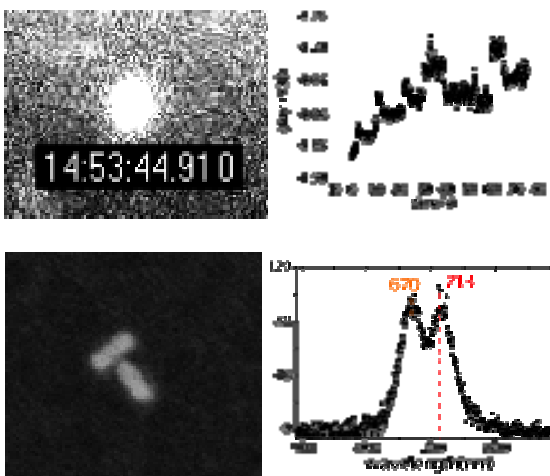


Fig. (Top) Optical trapping of gold nanospheres (Bottom) Optical trapping of gold nanorods

Characterizing the Effect of Substrate Stiffness on Neural Stem Cell Differentiation: Colleen T. Curley, Kristen Fanale, Ming-Tzo Wei, Daniel Ou-Yang, Dimitrios Vavylonis, Sabrina S. Jedlicka (ssj207@lehigh.edu) Lehigh University. Mechanical properties of the extracellular environment have been shown to influence stem cell maintenance and differentiation, however, the effects of substrate mechanics on neuronal differentiation are not clear. Differentiated neurons (dorsal root ganglia and cortical neurons) have been shown to develop longer neurite extensions on softer materials than stiffer ones, but previous studies do not address the ability of neurons to differentiate as a result of material elasticity. In this study, we characterize neuronal differentiation of C17.2 neural stem cells on polyacrylamide gels of variable stiffness. C17.2 neural stem cells were seeded onto polyacrylamide gels coated with Type I collagen, at a density of 10,000 cells/cm². The cells were then serum starved over a 14 day period, at which point the cells were fixed and analyzed for biochemical markers of differentiation. We have found that extent of C17.2 cell differentiation is dependent upon substrate stiffness, with softer polyacrylamide surfaces (100 Pa) leading to increased populations of neurons and increased neurite length. The next phase of the research will involve the quantification of synapse formation between C17.2 neurons on materials of variable stiffness, which would further support our claim that neural stem cells should differentiate to a greater degree on softer matrices.

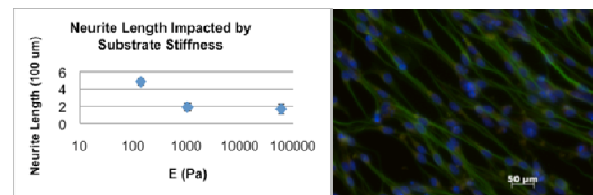


Fig. 1 Neurite length, measured with ImageJ, is affected by substrate stiffness

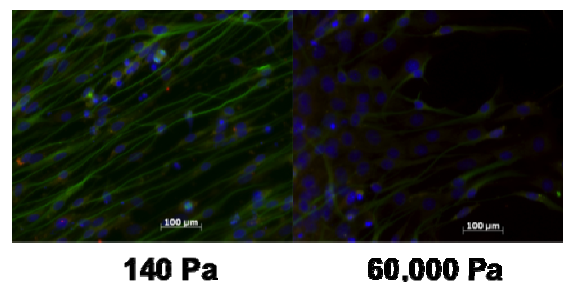


Fig. 2 Neural stem cells differentiated on soft vs. hard substrates.

Plasmonic Mach-Zehnder Interferometer for Ultrasensitive On-Chip Biosensing: Y. Gao, Q. Gan, Z. Xin, X. Cheng, and F. J. Bartoli (fjb205@lehigh.edu) *Lehigh University*. A plasmonic Mach-Zehnder interferometer (MZI) was experimentally demonstrated for miniaturized and ultrasensitive optical biosensing. The MZI is formed by patterning two parallel nanoslits in a thin metal film, and the sensor monitors the phase difference, modulated by surface biomolecular adsorptions, between surface plasmon waves propagating on top and bottom surfaces of the metal film. The combination of a nanoplasmonic architecture and sensitive interferometric techniques in this compact sensing platform yields an enhanced refractive index sensitivity S greater than 3500 nm/RIU and a record high sensing figure of merit ($S/\text{linewidth}$) exceeding 200 in the visible region, largely surpassing previous plasmonic sensors. We demonstrate real-time, label-free, quantitative monitoring of streptavidin-biotin specific binding with high signal-to-noise ratio in this simple, ultrasensitive, and miniaturized plasmonic biosensor.

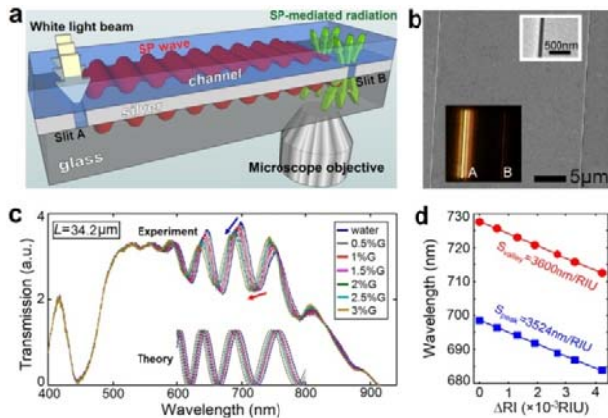


Fig. 1. (a) Schematic of the plasmonic MZI. (b) SEM image of a two-nanoslit structure with a slit separation of 22.7 μm . The upper inset shows a detailed SEM image of a slit (0.1 μm width). The lower inset shows a transmission image of two-nanoslit structure with only slit A being illuminated. (c) Measured spectra (upper curves) and calculated interference patterns (lower dotted curves) of plasmonic MZI with $L=34.2 \mu\text{m}$ for different glycerol-water solutions (glycerol volume concentration from 0% to 3%). The directions of the upper blue and lower red arrows indicate the blue-shifts of the peak and the valley. (d) Spectral position of the interference peak (squares) and valley (dots) versus refractive index change of the solutions. The solid lines are linear fits to the data.

Lateral Optical Binding Forces between Two Colloidal Mie Particles Trapped by Dual Highly Focused Laser Beams: Ming-Tzo Wei¹, Jack Ng², C. T. Chan², and H. Daniel Ou-Yang¹. ¹*Lehigh University, USA*, ²*Hong Kong University of Science and Technology, Hong Kong*. When submerged in a laser field, micro-particle cluster is subject to optical binding forces which can crystallize particles into a single piece of structure. Owing to Mie particles, the electromagnetic description of this optical binding force is beyond the dipole approximation. Here we report measurements and simulations of the purely lateral optical binding force between two Mie particles. We prove that the lateral optical binding force oscillates with the inter particle separation as well as phases retardation due to the interference of scattered field. The measured the oscillatory lateral optical binding forces under optical fields of different polarization exhibit multi-stabilities and a long interaction range in quantitative agreement with *ab initio* rigorous simulation.

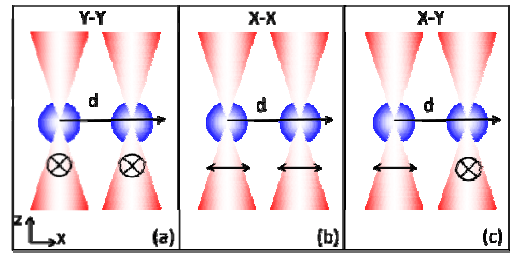


Fig. 1: Schematic illustration of the experimental configurations. In (a), (b) and (c), the polarizations of the incident beams are, respectively, perpendicular (Y-Y configuration), parallel (X-X configuration), and crossing (X-Y configuration) to the separation vector of the two particles.

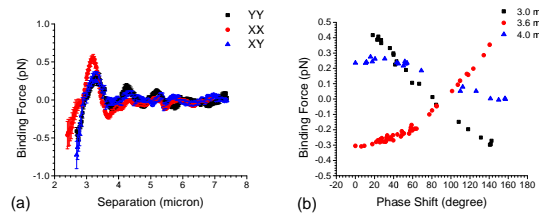


Fig. 2. (a) Experimental measurements of optical binding force as a function of separation for two 1.5 μm polystyrene particles trapped in a dual beam optical trap. (b) Optical binding force as function of relative phase between the two optical traps. Blue, red, and green correspond to separations of 3, 3.6, and 4.2 μm respectively.

Stress Fiber Organization and Dynamics in Cells Adhered to Substrates of Varying Stiffness: Wei Nie, Ming-Tzo Wei, H. Daniel Ou Yang, S. Jedlicka, Dimitrios Vavylonis (vavylonis@lehigh.edu) *Lehigh University*. Cellular morphology, locomotion and division are closely related to the stiffness of the substrates onto which the cells are cultured. The stiffness of cultured cells typically increases with the stiffness of the substrate. This increase correlates with increased contractility and the development of a meshwork of parallel and cross-linked stress fibers along the contacting surface. Many questions remain regarding the mechanisms that underlie cell-level cytoskeletal remodeling during mechanosensing. To better quantify the morphology and dynamics of the actomyosin cytoskeleton as a function of substrate stiffness, we cultured cells on polyacrylamide substrates coated with collagen I, with stiffness ranging from 1.05 kPa to 60 kPa (see Fig (a)). We used image segmentation methods to measure stress fiber and cortical myosin distributions in static 3D images. Time-lapse recordings show a connected stress fiber meshwork that evolves through new stress fiber formation on the cell periphery, contractile activity, and stress fiber merging and splitting over times of order hours. Figure (b) shows the MRLC-GFP intensity profile along a stress fiber during 40minutes.

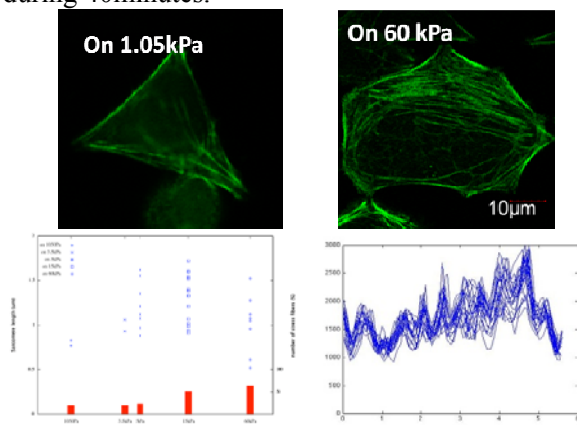


Fig. Quantitative analysis is suggestive of kinetic models that explore how different cortical myosin remodeling kinetics may contribute to different cell shape and rigidity depending on substrate stiffness.

Photophysics of Cy3-encapsulated Calcium Phosphate Nanoparticles: Hari S. Muddana, Thomas T. Morgan, James H. Adair, and Peter J. Butler (pjbbio@engr.psu.edu) *Penn State University*. Progress toward clinical application of

biodegradable fluorescent calcium phosphate (CP) nanoparticles as a bioimaging agent requires detailed knowledge of chromophore interaction with CP. As readouts of this cargo-matrix interaction, we determined the principle photophysical properties of Cy3 encapsulated in CP nanoparticles (CPNPs) using steady-state and time-resolved fluorescence spectroscopy. Fluorescence correlation spectroscopy (FCS)-determined diffusion coefficients and associated hydrodynamic radii confirmed the presence of highly monodisperse CPNPs with radii ranging from 7 to 10 nm. Single CP nanoparticles were 20 times brighter than free dye molecules because of a CP-induced 5-fold increase in quantum efficiency and encapsulation of four dye molecules per particle. Solvatochromic shifts resulting from hydrogen bonding between free dye and solvent or restricted intramolecular mobility by solvent viscosity were absent when Cy3 was encapsulated in CP. Encapsulation-mediated increases in radiative decay rates and decreases in nonradiative decay rates resulting in longer fluorescence lifetimes of Cy3 were attributed to solvent and CP-related local refractive indices and restricted flexibility of dye by rigid CP. Enhanced brightness of CPNPs enabled imaging of single nanoparticles under epifluorescence using both standard and total internal reflection fluorescence (TIRF) modes with camera exposure times on the order of tens of milliseconds. These enhanced photophysical properties together with excellent biocompatibility make CPNPs ideal for bioimaging applications ranging from single-molecule tracking to in vivo tumor detection and offer the possibility of timed codelivery of drugs to control cell function.

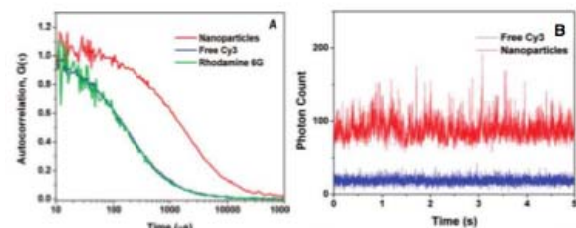


Fig. (A) Normalized autocorrelation of fluorescence fluctuations of CP nanoparticles (red), free Cy3 dye (blue), and rhodamine 6G (green). Shift of the curve to the right signifies smaller diffusion coefficient and larger hydrodynamic radius. (B) Representative raw fluorescence intensity signals from free Cy3 (blue) and CP nanoparticles (red) in PBS. Larger fluorescence fluctuations about the average indicates higher molecular brightness.

Mapping AC Electroosmotic Flow at the Dielectrophoresis Crossover Frequency of a Colloidal Probe

Jingyu Wang, H. Daniel Ou-Yang (hdo0@lehigh.edu) *Lehigh University* The AC electroosmosis (ACEO) flow field in the vicinity of conducting electrodes is mapped by the measurement of Stokes-Einstein forces on an optically trapped colloidal particle. Dielectrophoresis (DEP) of the probe particle is eliminated by measuring at the particle's DEP crossover frequency. At this frequency the DEP force on the particle vanishes. Isolation of ACEO from DEP of the probe utilizes the fact that the ACEO flow velocity depends strongly on the electric field, which is spatially dependent, whereas the DEP crossover frequency, is independent of the electric field. Elimination of the particle's DEP permits unambiguous mapping of the ACEO velocity field.

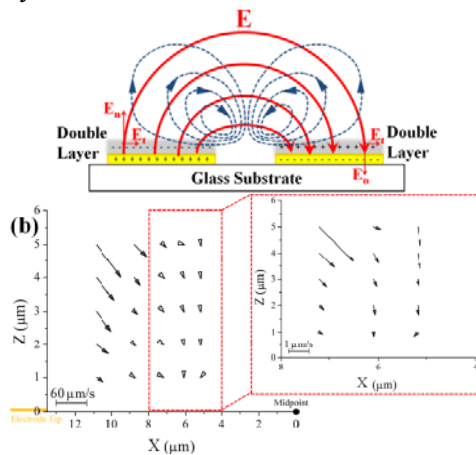


Fig. (a) Side view (not to scale) of symmetric AC electroosmotic flow (dashed lines) induced in an external AC electric field. The direction of the flow is indicated by the blue arrows. Solid lines show the electric field during a half cycle of the AC electric field generated by oppositely charged planar electrodes (yellow bars). The tangential and normal components of the electric field are indicated by red arrows (b) ACEO velocity field in the X-Z plane.

Low-frequency Dielectrophoretic Response of a Single Particle in Aqueous Suspensions

Jingyu Wang, H. Daniel Ou-Yang (hdo0@lehigh.edu) *Lehigh University*. α -relaxation, the counterion diffusion in the electric double layer, has been used to describe the anomalous low frequency dielectric dispersion of aqueous suspensions of colloidal particles. A microscopic theory describing this relaxation process proposed by Schwarz, however,

has not been investigated systematically. We propose to use a single particle dielectrophoretic (DEP) force spectroscopy to study the relaxation mechanism as a function of particle size, medium viscosity and temperature. DEP is a phenomenon of directed motion of electrically polarizable particles in a nonuniform AC electric field. As the frequency of the field is varied, the polarizability of the particle together with its associated double layer relative to the surrounding medium determines the magnitude and direction of the DEP force on the particle. The frequency at which the DEP force is zero is called the crossover frequency. Here we measure the dependence of the DEP crossover frequency and compare results with predictions by Schwarz.

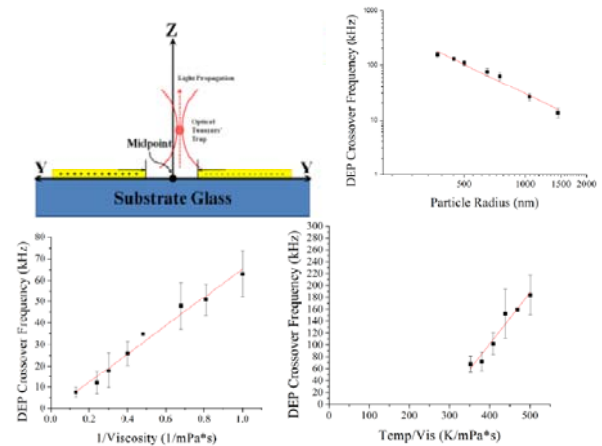


Fig. (a) Side view of the optical tweezers-based motion detection. (b) DEP crossover frequency as a function of particle size at the temperature of 25°C (c) DEP crossover frequency as a function of solvent viscosity at the temperature of 30°C (d) DEP crossover frequency as a function of the ratio of temperature/viscosity.

Ensemble Method to Measure the Potential Energy of Nanoparticles in an Optical Trap

Joseph Junio,¹ Jack Ng,² Joel A. Cohen,³ Zhifang Lin,⁴ and H. Daniel Ou-Yang¹ (hdo0@lehigh.edu) ¹*Lehigh University*, ²*Hong Kong University of Science and Technology*, ³*University of the Pacific, San Francisco*, ⁴*Fudan University*. A method is described for measuring the potential energy of nanoparticles in an optical trap by trapping an ensemble of particles with a focused laser beam. The force balance between repulsive osmotic and confining gradient-force pressures determines the single-particle trapping potential independent of interactions between the particles. The ensemble

nature of the measurement permits evaluation of single-particle trapping energies much smaller than $k_B T$. Energies obtained by this method are compared to those of single-particle methods as well as to theoretical calculations based on classical electromagnetic optics.

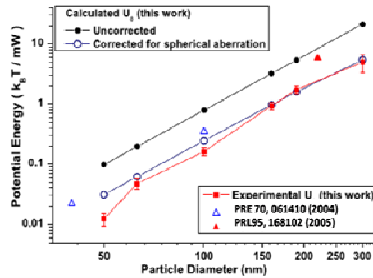


Fig. Experimental and calculated values of U_0 per milliwatt of laser power versus particle size. The refractive-index mismatch between the coverslip and the water was accounted for in the calculation

Elastic Response of Binary Hard-Sphere Fluids:

J. M. Rickman and H. Daniel Ou-Yang (hdo0@lehigh.edu) *Lehigh University*. We derive expressions for the high-frequency, wave-number-dependent elastic constants of a binary hard-sphere fluid and employ Monte Carlo computer simulation to evaluate these constants in order to highlight the impact of composition and relative sphere diameter on the elastic response of this system. It is found that the elastic constant $c_{11}(k)$ exhibits oscillatory behavior as a function of k whereas the high-frequency shear modulus, for example, does not. This behavior is shown to be dictated by the angular dependence (in k space) of derivatives of the interatomic force at contact. The results are related to recent measurements of the compressibility of colloidal fluids in laser trapping experiments.

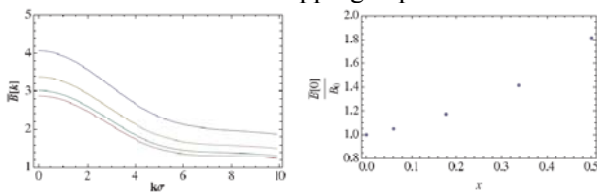


Fig. (a) The normalized, infinite-wavelength bulk modulus, $B(k)$, versus the normalized wavenumber, $k\sigma$, with $\alpha = 0.414$. The curves, from top to bottom, correspond to the compositions $x = 0.339, 0.178, 0.060,$ and 0.0 , respectively. (b) The normalized, infinite-wavelength bulk modulus, $B(k = 0)/B_0$, where B_0 is the corresponding modulus for $x = 0$, versus composition, x , for a binary hard-sphere fluid with $\alpha = 0.414$.

Principal Investigators

Filbert J. Bartoli, Lehigh University
Email: fjb205@lehigh.edu

Ivan Biaggio, Lehigh University
Email: ivb2@lehigh.edu

Peter J. Butler, Penn State University
Email: pjbbio@engr.psu.edu

Xuanhong Cheng, Lehigh University
Email: xuc207@lehigh.edu

Volkmar Dierolf, Lehigh University
Email: vod2@lehigh.edu

Sabrina S. Jedlicka, Lehigh University
Email: ssj207@lehigh.edu

H. Daniel Ou-Yang, Lehigh University
Email: hdo0@lehigh.edu

Dimitrios Vavylonis, Lehigh University
Email: vavylonis@lehigh.edu